Knockdown of AMP-activated protein kinase α2 impairs epithelial-mesenchymal transition in rat renal tubular epithelial cells by downregulating v-ets erythroblastosis virus E26 oncogene homolog-1 and ribosomal protein S6 kinase A1

Xiaoming Yin [1], **Fujiang Ma** [2], **Xu Fan** [1], **Qi Zhao** [1], **Xin Liu** [1], **Yi Yang** [Corresp. 1]

[1] Department of Pediatric Urology, Shengjing Hospital of China Medical University, Shenyang, Liaoning, China

[2] Tianjin children's hospital, Tianjin, Hebei, China

Corresponding Author: Yi Yang
Email address: yangy2@sj-hospital.org

Background. Epithelial mesenchymal transition (EMT) plays an important regulatory role in obstructive nephropathy and renal fibrosis. As an intracellular energy sensor, AMP-activated protein kinase (AMPK) is essential in the process of EMT. The aim of this study was to reveal changes in the expression of AMPKα2 and to elucidate which AMPKα2 genes play a role during EMT. **Methods.** In this study, TGF-β1 was used to induce EMT in normal rat renal tubular epithelial (NRK-52E) cells. The shAMPKα2 lentivirus was used to interfere with AMPKα2 expression in EMT-derived NRK-52E cells, where AMPKα2 expression and EMT were detected. Differential gene expression after the AMPKα2 knockdown in EMT-derived NRK-52E cells was examined using a gene microarray. Possible regulatory pathways were analyzed using ingenuity pathway analysis (IPA) and differentially expressed genes were partially verified by quantitative real-time polymerase chain reaction (qRT-PCR) and western blotting. **Results.** It was found that AMPKα2 was upregulated in TGF-β1-induced EMT-derived NRK-52E cells. EMT progression was significantly inhibited after the expression of AMPKα2 was downregulated by the shAMPKα2 lentivirus. A total of 1,588 differentially expressed genes were detected after the AMPKα2 knockdown in NRK-52E cells in which EMT occurred. The ERK/MAPK pathway was significantly impaired after the AMPKα2 knockdown, as indicated by the IPA analysis. Furthermore, qRT-PCR and western blot results revealed that the expression of AMPKα2, v-ets erythroblastosis virus E26 oncogene homolog-1 (ETS1), and ribosomal protein S6 kinase A1 (RPS6KA1) was upregulated after EMT in NRK-52E cells, while expression of ETS1 and RPS6KA1 was downregulated after the AMPKα2 knockdown. **Conclusions.** AMPKα2 plays an important role in the regulation of rat renal tubular EMT, which may be achieved by modulating ETS1 and RPS6KA1 in the ERK/MAPK pathway.

Knockdown of AMP-activated protein kinase α2 impairs epithelial-mesenchymal transition in rat renal tubular epithelial cells by downregulating v-ets erythroblastosis virus E26 oncogene homolog-1 and ribosomal protein S6 kinase A1

Xiaoming Yin [1], Fujiang Ma [2], Xu Fan [1], Qi Zhao [1], Xin Liu[1], Yi Yang [1,]

[1] Division of Pediatric Urology, Shengjing Hospital of China Medical University, Shenyang, Liaoning, China.

[2] Department of Pediatric Urology, Tianjin children's hospital, Tianjin, Hebei, China.

Corresponding Author:
Yi Yang [1]
No.36 Sanhao Street, Shenyang, Liaoning 110004, China.
Email address: yangy2@sj-hospital.org

Abstract

Background. Epithelial mesenchymal transition (EMT) plays an important regulatory role in obstructive nephropathy and renal fibrosis. As an intracellular energy sensor, AMP-activated protein kinase (AMPK) is essential in the process of EMT. The aim of this study was to reveal changes in the expression of AMPKα2 and to elucidate which AMPKα2 genes play a role during EMT.

Methods. In this study, TGF-β1 was used to induce EMT in normal rat renal tubular epithelial (NRK-52E) cells. The shAMPKα2 lentivirus was used to interfere with AMPKα2 expression in EMT-derived NRK-52E cells, where AMPKα2 expression and EMT were detected. Differential gene expression after the AMPKα2 knockdown in EMT-derived NRK-52E cells was examined using a gene microarray. Possible regulatory pathways were analyzed using ingenuity pathway analysis (IPA) and differentially expressed genes were partially verified by quantitative real-time polymerase chain reaction (qRT-PCR) and western blotting.

Results. It was found that AMPKα2 was upregulated in TGF-β1-induced EMT-derived NRK-52E cells. EMT progression was significantly inhibited after the expression of AMPKα2 was downregulated by the shAMPKα2 lentivirus. A total of 1,588 differentially expressed genes were detected after the AMPKα2 knockdown in NRK-52E cells in which EMT occurred. The ERK/MAPK pathway was significantly impaired after the AMPKα2 knockdown, as indicated by the IPA analysis. Furthermore, qRT-PCR and western blot results revealed that the expression of AMPKα2, v-ets erythroblastosis virus E26 oncogene homolog-1 (ETS1), and ribosomal protein S6 kinase A1 (RPS6KA1) was upregulated after EMT in NRK-52E cells, while expression of ETS1 and RPS6KA1 was downregulated after the AMPKα2 knockdown.

Conclusions. AMPKα2 plays an important role in the regulation of rat renal tubular EMT, which may be achieved by modulating ETS1 and RPS6KA1 in the ERK/MAPK pathway.

Introduction

Ureteropelvic junction obstruction is the most common obstructive urinary tract disease in pediatric urology division, with an incidence of 0.5/1,000–1/1,000 (Weitz et al. 2016) . It is also one of the causes of obstructive nephropathy characterized by renal fibrosis (Klahr 2000). The main features of this irreversible renal fibrosis are glomerular sclerosis and tubulointerstitial fibrosis (Shihab 2007). Recent studies have found that tubulointerstitial fibrosis is closely related to the process of epithelial mesenchymal transition (EMT) (Iwano 2010). EMT is characterized by a loss of adhesion and polarity of epithelial cells and induction of α-smooth muscle actin (α-

SMA) (Martin-Belmonte & Perez-Moreno 2011; Puisieux et al. 2014). EMT is involved in many pathological changes, including fibrosis and tumor metastasis (Bronsert et al. 2014; Liu 2011). The transforming growth factor-β (TGF-β) signaling pathway plays an important role in regulation of renal fibrosis (Kim & Choi 2012). TGF-β1 expression is significantly upregulated in the process of renal fibrosis caused by unilateral ureteral obstruction (Zhang et al. 2010).

We identified several proteins with differential expression between rat kidney tissues from sham operated group and those with complete unilateral ureteral obstruction. These identified proteins were reported to be involved in cell apoptosis, energy metabolism and injuries of mitochondrion and oxidative stress in the preliminary study(Zhao et al.). AMP-activated protein kinase (AMPK), including α1/2, β1/2, and γ1/2/3 subunits, is a mitochondrial energy sensor that senses changes in AMP levels. AMPK is involved in the maintenance of cellular energy balance by affecting multiple factors during metabolism (Jeon 2016). Increased intracellular ratio of AMP to ATP activates AMPK, while AMP binds to the AMPK γ subunit, causing conformational changes in the protein and allowing phosphorylation of the Thr-172 site in the α subunit (Hawley et al. 2003). Recent studies have shown that AMPK, especially AMPKα2, can regulate EMT processes during liver and kidney fibrosis (Qiu et al. ; Wang et al. 2016; Wang et al. 2010) and play an important role in tumor cell metastasis (Saxena et al. 2018). However, the underlying mechanisms for AMPK changes in renal tubular EMT remain unclear.

In this study, the expression of AMPKα2 in EMT-derived normal rat renal tubular epithelial (NRK-52E) cells induced by TGF-β1 was investigated. Gene microarray was used to analyze differential gene expression in EMT-derived NRK-52E cells before and after the AMPKα2 knockdown. Ingenuity pathway analysis (IPA) was performed to reveal specific genes and signaling pathways involved in the regulation of EMT by AMPKα2. Finally, quantitative real-time polymerase chain reaction (qRT-PCR) and western blotting were used to verify the prediction results.

Materials & Methods

1. Cell Culture, RNA Interference, and TGF-β1 EMT Induction

The NRK-52E cells (Baihaobio, Liaoning, China) were cultured in Dulbecco's Modified Eagle's Medium (DMEM/high glucose; ca. no.SH30022.01; Hyclone, UT, USA) supplemented with 10% fetal bovine serum (FBS) (ca. no.SH30071.03; Hyclone, UT, USA) and 3% penicillin-streptomycin solution (ca. no.SV30010; Hyclone, UT, USA). Cell culture was maintained at 37°C in a humidified atmosphere at 5% CO_2. Cell medium was changed every 2 days.

The sequence of siRNA(5'-GCTGACTTCGGACTCTCTA-3') was designed by GeneChem Co., Ltd. (Shanghai, China) for targeting the AMPKα2 sequence(GenBank no. NM_023991). The AMPKα2 hairpin oligonucleotide was inserted into the GV248-GFP lentiviral vector (GeneChem Co., Ltd.) to construct a GV248-GFP-short hairpin AMPKα2 (sh AMPKα2) AMPKα2-knockdown vector. The negative control (shCtrl) sequence was 5'-TTCTCCGAACGTGTCACGT-3', and when incorporated into the lentiviral vector was referred to as GV248-GFP-shCtrl. The NRK-52E cells were transfected with AMPKα2 short hairpin RNA (shRNA) lentivirus (LV) or control LV according to the manufacturer's protocol (GeneChem, Shanghai, China). NRK52-E cells with a stable AMPKα2 knockdown (KD) were established. The efficacy of AMPKα2 KD was validated using a qRT-PCR.

For the TGF-β1 treatment, all cells were stimulated with 10 ng/mL recombinant TGF-β1 (Proteintech Group, IL,USA) for 24 h. Cells were divided into four groups as follows: negative control, TGF-β1-treated, TGF-β1-treated+ shCtrl, and TGF-β1-treated+shAMPKα2 KD. Protein expression and location were determined using immunofluorescence staining. Total RNA was extracted and analyzed using qRT-PCR. Proteins extracted from total cell lysates were analyzed using western blotting. All measurements were replicated at least three times.

2. Gene Microarray

The genome-wide effect of AMPKα2 KD was studied using the GeneChip™ Rat Genome 2302.0 Array (Affymetrix; Thermo Fisher Scientifc, Inc., MA, USA) consisting of 28,000 genes. Three biological replicates of EMT-derived NRK-52E cells transduced with shAMPKα2 or shCtrl LV (for 72 h) were analyzed using a microarray. RNA was initially isolated using the TRIzol reagent and its quality was determined using the NanoDrop 2000 spectrophotometer (NanoDrop; Thermo Fisher Scientific,Inc., DE, USA) and Agilent Bioanalyzer 2100 (Agilent Technologies, Inc., CA, USA). Individual microarrays were used for gene expression profiling of each sample. Briefly, 500 ng samples of RNA were reverse-transcribed and labeled with biotin using the GeneChip3' IVT labeling kit according to the manufacturer's protocol. Labeled cDNA was then hybridized onto the GeneChip™Rat Genome 230 2.0 Array. Arrays were performed with the GeneChip®Hybridization, Wash, and Stain kit using the GeneChip® Fluidics Station 450. All of the GeneChip® products were obtained from Affymetrix, Thermo Fisher Scientific, Inc. and used according to the manufacturer's protocol. The chip array was scanned directly post-hybridization using the GeneChip® Scanner 3000. Microarray data were analyzed using the

GeneSpring software (version 11; Agilent Technologies, Inc., CA, USA). In this study, P-values were determined using a linear model based on the empirical Bayesian distribution (Ritchie et al. 2015). The false discovery rate (FDR) was corrected using the Benjamini-Hochberg method. The screening criteria for significantly differential genes were: |Fold Change|>3 and FDR<0.05.

3. IPA

Datasets representing differentially expressed genes derived from the microarray analyses were imported into the IPA tool (http://www.ingenuity.com; Ingenuity® Systems, CA, USA). The "core analysis" function in the IPA software was used to interpret differentially expressed data, which included functional signaling pathways. Differentially expressed genes were mapped onto functional signaling pathways available in the Ingenuity database. Z-score activation algorithms were computed using the IPA software. Analyses performed within the IPA program included identification of a particular dataset and its functional signaling pathways in accordance with the purpose of the present study.

4. qRT-PCR

Total RNA was isolated from the NRK-52E cells using RNAiso Plus (TaKaRa Biotech, Shiga, Japan) according to the manufacturer's instructions and subjected to reverse transcription into cDNA with the PrimeScript™ RT Reagent Kit (TaKaRa Biotech, Shiga, Japan). The qRT-PCR analysis was performed using the ABI ViiA7DX System (Applied Biosystems, CA, USA). The β-actin expression was used as an internal reference for all PCR experiments. Primers of qRT-PCR designed for specific target genes were synthesized by TaKaRa Biotech(Shiga, Japan) (Table 1). PCR reactions were performed using the following cycling conditions: 95°C for 30 s, followed by 40 cycles of 95°C for 5 s, 60°C for 30 s, and 72°C for 20 s. The relative mRNA levels for each sample were calculated by the $2^{-\Delta\Delta ct}$ method.

5. Western Blot Analysis

Proteins were isolated using an isolation kit (RIPA Lysis Buffer [50mM Tris (pH 7.4)，150mM NaCl， 1% NP-40，0.5% sodium deoxycholate，0.1% SDS] and 1mM PMSF)from Beyotime Institute of Biotechnology (Shanghai, China) according to the manufacturer's instructions and quantified using the 2D-Quant kit. A total of 50 μg of protein extracted from the cells was separated by 8% sodium dodecyl sulfate-polyacrylamide gel electrophoresis and then transferred in Tris-HCl methanol (20 mM Tris, 150 mM glycine, and 20% methanol) onto polyvinylidene difluoride membranes (EMD Millipore, MA, USA) using a Trans-Blot

electrophoresis transfer cell (Bio-Rad, CA, USA). The membranes were subsequently blocked with 5% non-fat dry milk in Tris-buffered saline containing 0.1% Tween (TBST) and incubated with primary antibodies overnight at 4˚C. Primary antibodies included AMPKα2 (polyclonal rabbit; 1:2,000 dilution; cat. no. ab3760; Abcam, Cambs, UK), v-ets erythroblastosis virus E26 oncogene homolog-1(ETS-1) (monoclonal rabbit; 1:1,000 dilution; cat. no. 14069S; Cell Signaling Technology, MA, USA), homolog-1 and ribosomal protein s6 kinase A1 (RPS6KA1) (monoclonal rabbit; 1:1,000 dilution; cat. no. ab32114; Abcam, Cambs, UK), E-cadherin (monoclonal mouse; 1:1,000 dilution; cat. no. 14472S; Cell Signaling Technology, MA, USA), α- SMA (monoclonal mouse; 1:100 dilution; cat. no. ab7817; Abcam, Cambs, UK), vimentin (monoclonal mouse; 1:1,000 dilution; cat. no. ab8978; Abcam, Cambs, UK), and glyceraldehyde-3-phosphate dehydrogenase (GAPDH) (monoclonal rabbit; 1:10,000 dilution; cat. no. ab181602; Abcam, Cambs, UK). After three washes in TBST (10 min/wash), the membranes were incubated with goat anti-rabbit immunoglobulin G (IgG)-horseradish peroxidase (HRP, 1:2,000 dilution; cat. no. ab6721; Abcam, Cambs, UK) or goat anti-mouse IgG-HRP (1:2,000 dilution; cat. no. ab275019; Abcam, Cambs, UK) secondary antibodies for 1 h at room temperature and were washed again. All immune blots were performed at least in triplicate. The antigen-antibody complexes were visualized using enhanced chemiluminescence reagents (Thermo Fisher Scientific, CA, USA). The GAPDH was as loading control. Detected bands were quantified using the ImageJ 2× software (version 2.1.4.7; National Institutes of Health, MD, USA). The relative density of each protein was calculated by dividing the optical density value of each protein by that of the loading control.

6. Immunofluorescence Staining

NRK-52E cells (1×10^6) were washed with phosphate buffer saline (PBS) and fixed in 4% paraformaldehyde for 30 min at room temperature. Fixed cells were washed again with PBS and permeabilized in 0.5% Triton X-100 diluted in PBS for 10 min. The cells on the slides were subsequently blocked with 5% bovine serum albumin (Beyotime Institute of Biotechnology, Shanghai, China) for 1 h at room temperature. Subsequently, the cells of negative control and aTGF-β1-treated groups incubated with the AMPKα2 antibody (polyclonal rabbit; 1:100 dilution; cat. no. ab3760; Abcam, Cambs, UK) at 4˚C overnight. The cells of aTGF-β1-treated+ shCtrl and TGF-β1-treated+shAMPKα2 KD groups incubated with the green fluorescent protein (GFP) antibody (polyclonal rabbit antibody; 1:2,000 dilution; cat. no. ab6556; Abcam, Cambs,

UK) at 4˚C overnight. They were then incubated with fluorescein isothiocyanate and rhodamine-conjugated goat anti-rabbit (cat. no. sc-2012; Santa Cruz Biotechnology, CA, USA) secondary antibodies at a 1:100 dilution. The 4',6-diamidino-2-phenylindole (DAPI, Bioss, Inc., Beijing, China) was used to stain the cell nuclei on glass slides. The cells were then examined using fluorescence microscopy (Nikon CE1 Confocal Microscope, Nikon, Tokyo, Japan).

7. Statistical Analysis

Statistical analysis was performed using Student's t-test or one-way ANOVA. Analysis was performed with the SPSS (version 23.0; SPSS, Inc., Chicago, IL, USA). P-values <0.05 were considered to indicate a statistically significant difference.

Results

1. AMPKα2 expression is upregulated after TGF-β1 induces EMT in NRK-52E cells and EMT is impaired in NRK-52E cells after AMPKα2 knockdown.

TGF-β1 was first applied to induce EMT in the NRK-52E cells. Resulting morphological changes in the NRK-52E cells included a change from a typical round and polygonal shape to a fusiform shape, suggesting that EMT occurred (Figure 1). In addition, western blot experiments showed that EMT protein markers α-SMA and vimentin were upregulated, while epithelial cell protein marker E-cadherin was downregulated, further confirming the occurrence of EMT (Figure 2).

Immunofluorescence experiments showed that AMPKα2 was mainly expressed in the cytoplasm and nucleus of NRK-52E cells (Figure 3A). Western blot and qRT-PCR experiments revealed that AMPKα2 protein and mRNA expression were significantly upregulated during EMT in NRK-52E cells (Figure4, 3B).

GFP expression was observed 72 h after the shAMPKα2 and shCtrl LV transfection in the NRK-52E cells that underwent EMT induced by TGF-β1, indicating that transfection was successful (Figure 5A). Expression of AMPKα2 mRNA was downregulated by 70% in the TGF-β1-treated+shAMPKα2 group compared to the TGF-β1-treated+shCtrl group in qRT-PCR results, indicating that AMPKα2 was specifically and effectively knocked down (Figure 5B). In addition, western blot experiments showed that expression of AMPKα2 protein was downregulated in the TGF-β1-treated+shAMPKα2 group compared to the TGF-β1-treated+shCtrl group. The expression of α-SMA and vimentin was downregulated, while E-cadherin expression was upregulated, suggesting that EMT process was inhibited after the

AMPKα2 knockdown (Figure 2). These data implied that AMPKα2 might play an important regulatory role in the process of EMT in NRK-52E cells.

2. Differential gene expression and IPA after AMPKα2 knockdown in NRK-52E cells with EMT

To detect which genes were changed after the AMPKα2 KD, gene expression profiles of EMT-derived NRK-52E cells transduced with shAMPKα2 or shCtrl-payload LVs were determined using the GeneChip Rat 230 2.0® PathArrayTM Rat Gene Expression Array with three biological replicates. A total of 1588 differentially expressed genes were identified, of which 1,510 were downregulated and 78 were upregulated (Figure 6A).

Next, IPA was applied to conduct pathway analysis of 1,588 differentially expressed genes. The IPA revealed that AMPKα2 may regulate EMT progression in NRK-52E cells via multiple pathways. According to the IPA internal algorithms and standards, a z-score>2 represents a significantly activated pathway, while a z-score<-2 represents a significantly inhibited pathway. In the present study, the ERK/MAPK pathway was significantly inhibited (z-score = -3.550, Figure 6B). Therefore, the AMPKα2 regulation of renal tubular epithelial EMT was achieved mainly via the ERK/MAPK pathway.

IPA results indicated that 36 genes were inhibited in the ERK/MAPK signaling pathway after the AMPKα2 knockdown (Table 2 and Figure 6C).

3. ETS1 and RPS6KA1 in ERK/MAPK signaling pathway were upregulated in NRK-52E cells with EMT, while ETS1 and RPS6KA1 were downregulated after AMPKα2 knockdown.

Five significantly inhibited genes, including HRAS, CRK, ETS1, RPS6KA1, and CREB1, were selected for validation. Using qRT-PCR, ETS1 and RPS6KA1 mRNA levels were found to be significantly upregulated in the TGF-β1-treated group compared to the negative control. The expression was significantly downregulated in the TGF-β1-treated+shAMPKα2 KD group compared to the TGF-β1-treated+shCtrl group (Figure 7). Inconsistent with microarray results, AMPKα2 downregulation has no effect on HRAS, CRK and CREB1. Western blot experiments showed that expression of ETS1 and RPS6KA1 proteins in the TGF-β1-treated group was significantly higher than that in the negative control. The expression was significantly lower in the TGF-β1-treated+shAMPKα2 KD group than that in the TGF-β1-treated+ shCtrl group (Figure 8,9). Therefore, AMPKα2 may act by regulating ETS1 and RPS6KA1 in the ERK/MAPK signaling pathway during EMT.

Discussion

Renal fibrosis is considered to be an irreversible process that eventually develops into end-stage renal failure. EMT plays an important role in obstructive nephropathy and renal fibrosis. Therefore, delay, prevention, and reversal of renal cell EMT are keys for the treatment of obstructive nephropathy (Grande & Lopez-Novoa 2009). In the current study, AMPKα2 played an important role in EMT of NRK-52E cells and was upregulated in the TGF-β1-induced EMT-derived NRK-52E cells. Interference with AMPKα2 expression by shAMPKα2 LV significantly impaired EMT progression. Moreover, using rat gene chip experiments and IPA, it was discovered that AMPKα2 may play an important role in EMT process by regulating ETS1 and RPS6KA1.

AMPK is an AMP-activated protein kinase that senses changes in AMP levels and maintains cell energy balance via multiple pathways that affect cellular metabolism, playing an important role in kidney disease (Tain & Hsu 2018). However, current research on the topic of promotion or inhibition of EMT after AMPK activation is controversial, which may be due to the biological or cellular specificity of AMPK. Hepatocyte EMT can cause liver fibrosis. The Wang et al. study in rat liver cells indicated that AMPK can promote hepatocyte EMT, while the use of AMPK-specific inhibitors can limit it (Wang et al. 2010). In addition, EMT can also promote tumor cell metastasis. Studies have shown that in breast cancer, lung cancer, and melanoma cells, AMPK activation can cause EMT, thereby promoting tumor cell metastasis (He et al. 2016; Saxena et al. 2018). The results from the current study are in line with these previous findings. However, other studies are contradictory to the idea that AMPK activation can reduce EMT. Previous research has shown that activation of AMPK can inhibit the trans-differentiation of myofibroblasts induced by TGF-β/smad3 and the occurrence of hepatic astrocytic fibrosis (Lim et al. 2012; Mishra et al. 2008). In addition, metformin can activate AMPK to inhibit the TGF-β signaling pathway and alleviate EMT process in rat kidneys in the model of renal ischemia-reperfusion injury in rats (Wang et al. 2016). These inconsistent results may be due to tissue specificity or distinct EMT models. In this study, TGF-β1 was used to induce EMT in NRK-52E cells, while the expression of AMPKα2 was up-regulated. EMT was inhibited after the LV AMPKα2 knockdown, indicating that AMPKα2 plays an important role in EMT of NRK-52E cells.

To investigate the expression of differential genes in EMT-derived NRK-52E cells before and after the AMPKα2 knockdown, high-throughput analysis was used. According to the gene chip and IPA results, genes in the ERK/MAPK pathway were strongly inhibited after the AMPKα2

down-regulation, indicating that AMPKα2 modulates renal tubular EMT by inhibiting the ERK/MAPK pathway. Five genes that were strongly inhibited in the ERK/MAPK pathway, including HRAS, CRK, ETS1, RPS6KA1, and CREB1, were selected for validation. Using qRT-PCR, ETS1 and RPS6KA1 were found to be highly expressed in EMT-derived NRK-52E cells. ETS1 and RPS6KA1 gene expression was decreased after the AMPKα2 knockout, which is consistent with the microarray results, indicating that AMPKα2 KD inhibits EMT by downregulating the ETS1 and RPS6KA1 genes. However, HRAS, CRK, and CREB1 verification results may not be consistent with the microarray results.

RPS6KA1 is a member of the serine threonine kinase family, which has an N-terminal and a C-terminal kinase domain. The C-terminal domain can be activated by ERK1/2 phosphorylation and calcium-dependent kinase. The activated RPS6KA1 phosphorylates CREB, NF-kb, and other transcription factors (Abe et al. 2017). RPS6KA1 can cause apoptosis of renal tubular epithelial cells during renal fibrosis (Lin et al. 2019), although EMT of renal tubular epithelial cells has not been reported yet. ETS1 is a downstream transcription factor of ERK (Plotnik et al. 2014). ETS1 is widely expressed in rat kidneys and its normal expression can ensure normal differentiation and development of the kidney (Lawrence et al. 2008). Some researchers have shown that ETS1 may play a role in the differentiation of liver cells via regulation of the ERK pathway (Paumelle et al. 2002). Therefore, both RPS6KA1 and ETS1 may play important regulatory roles in the renal tubular EMT, although the underlying mechanism and relationship between AMPKα2 and its regulation need further study.

Some limitations were present in this study. Subsequent experiments need to further verify whether AMPKα2 similarly regulates RPS6KA1 and ETS1 in human renal tubular epithelial cells, whether AMPKα2 phosphorylation occurs during the renal tubular EMT, and how AMPKα2 regulates RPS6KA1 and ETS1 in the renal tubular EMT. Nevertheless, the current study was first to demonstrate that AMPKα2 KD may impair renal tubular EMT by inhibiting the expression of RPS6KA1 and ETS1.

Conclusions

In summary, AMPKα2 plays an important regulatory role in the rat renal tubular EMT and this regulation may be achieved by modulating ETS1 and RPS6KA1 in the ERK/MAPK pathway. However, specific AMPKα2 regulation of ETS1 and RPS6KA1 requires further study.

Acknowledgements

We give special thanks to all the teachers in the Division of Pediatric Urology at Shengjing Hospital of China Medical University for their help and support.

References

Abe JI, Sandhu UG, Hoang NM, Thangam M, Quintana-Quezada RA, Fujiwara K, and Le NT. 2017. Coordination of Cellular Localization-Dependent Effects of Sumoylation in Regulating Cardiovascular and Neurological Diseases. *Adv Exp Med Biol* 963:337-358. 10.1007/978-3-319-50044-7_20

Bronsert P, Enderle-Ammour K, Bader M, Timme S, Kuehs M, Csanadi A, Kayser G, Kohler I, Bausch D, Hoeppner J, Hopt UT, Keck T, Stickeler E, Passlick B, Schilling O, Reiss CP, Vashist Y, Brabletz T, Berger J, Lotz J, Olesch J, Werner M, and Wellner UF. 2014. Cancer cell invasion and EMT marker expression: a three-dimensional study of the human cancer-host interface. *J Pathol* 234:410-422. 10.1002/path.4416

Grande MT, and Lopez-Novoa JM. 2009. Fibroblast activation and myofibroblast generation in obstructive nephropathy. *Nat Rev Nephrol* 5:319-328. 10.1038/nrneph.2009.74

Hawley SA, Boudeau J, Reid JL, Mustard KJ, Udd L, Makela TP, Alessi DR, and Hardie DG. 2003. Complexes between the LKB1 tumor suppressor, STRAD alpha/beta and MO25 alpha/beta are upstream kinases in the AMP-activated protein kinase cascade. *J Biol* 2:28. 10.1186/1475-4924-2-28

He K, Guo X, Liu Y, Li J, Hu Y, Wang D, and Song J. 2016. TUFM downregulation induces epithelial-mesenchymal transition and invasion in lung cancer cells via a mechanism involving AMPK-GSK3beta signaling. *Cell Mol Life Sci* 73:2105-2121. 10.1007/s00018-015-2122-9

Iwano M. 2010. EMT and TGF-beta in renal fibrosis. *Front Biosci (Schol Ed)* 2:229-238.

Jeon SM. 2016. Regulation and function of AMPK in physiology and diseases. *Exp Mol Med* 48:e245. 10.1038/emm.2016.81

Kim SI, and Choi ME. 2012. TGF-beta-activated kinase-1: New insights into the mechanism of TGF-beta signaling and kidney disease. *Kidney Res Clin Pract* 31:94-105. 10.1016/j.krcp.2012.04.322

Klahr S. 2000. Obstructive nephropathy. *Intern Med* 39:355-361. 10.2169/internalmedicine.39.355

Lawrence MC, McGlynn K, Shao C, Duan L, Naziruddin B, Levy MF, and Cobb MH. 2008. Chromatin-bound mitogen-activated protein kinases transmit dynamic signals in transcription complexes in beta-cells. *Proc Natl Acad Sci U S A* 105:13315-13320. 10.1073/pnas.0806465105

Lim JY, Oh MA, Kim WH, Sohn HY, and Park SI. 2012. AMP-activated protein kinase inhibits TGF-beta-induced fibrogenic responses of hepatic stellate cells by targeting transcriptional coactivator p300. *J Cell Physiol* 227:1081-1089. 10.1002/jcp.22824

Lin L, Shi C, Sun Z, Le NT, Abe JI, and Hu K. 2019. The Ser/Thr kinase p90RSK promotes kidney fibrosis by modulating fibroblast-epithelial crosstalk. *J Biol Chem*. 10.1074/jbc.RA119.007904

Liu Y. 2011. Cellular and molecular mechanisms of renal fibrosis. *Nat Rev Nephrol* 7:684-696. 10.1038/nrneph.2011.149

Martin-Belmonte F, and Perez-Moreno M. 2011. Epithelial cell polarity, stem cells and cancer. *Nat Rev Cancer* 12:23-38. 10.1038/nrc3169

Mishra R, Cool BL, Laderoute KR, Foretz M, Viollet B, and Simonson MS. 2008. AMP-activated protein kinase inhibits transforming growth factor-beta-induced Smad3-dependent transcription and myofibroblast transdifferentiation. *J Biol Chem* 283:10461-10469. 10.1074/jbc.M800902200

Paumelle R, Tulasne D, Kherrouche Z, Plaza S, Leroy C, Reveneau S, Vandenbunder B, and Fafeur V. 2002. Hepatocyte growth factor/scatter factor activates the ETS1 transcription factor by a RAS-RAF-MEK-ERK signaling pathway. *Oncogene* 21:2309-2319. 10.1038/sj.onc.1205297

Plotnik JP, Budka JA, Ferris MW, and Hollenhorst PC. 2014. ETS1 is a genome-wide effector of RAS/ERK signaling in epithelial cells. *Nucleic Acids Res* 42:11928-11940. 10.1093/nar/gku929

Puisieux A, Brabletz T, and Caramel J. 2014. Oncogenic roles of EMT-inducing transcription factors. *Nat Cell Biol* 16:488-494. 10.1038/ncb2976

Qiu S, Xiao Z, Piao C, Zhang J, Dong Y, Cui W, Liu X, Zhang Y, and Du J. AMPKalpha2 reduces renal epithelial transdifferentiation and inflammation after injury through interaction with CK2beta.

Ritchie ME, Phipson B, Wu D, Hu Y, Law CW, Shi W, and Smyth GK. 2015. limma powers differential expression analyses for RNA-sequencing and microarray studies. *Nucleic Acids Res* 43:e47. 10.1093/nar/gkv007

Saxena M, Balaji SA, Deshpande N, Ranganathan S, Pillai DM, Hindupur SK, and Rangarajan A. 2018. AMP-activated protein kinase promotes epithelial-mesenchymal transition in cancer cells through Twist1 upregulation. *J Cell Sci* 131. 10.1242/jcs.208314

Shihab FS. 2007. Do we have a pill for renal fibrosis? *Clin J Am Soc Nephrol* 2:876-878. 10.2215/cjn.02660707

Tain YL, and Hsu CN. 2018. AMP-Activated Protein Kinase as a Reprogramming Strategy for Hypertension and Kidney Disease of Developmental Origin. *Int J Mol Sci* 19. 10.3390/ijms19061744

Wang M, Weng X, Guo J, Chen Z, Jiang G, and Liu X. 2016. Metformin alleviated EMT and fibrosis after renal ischemia-reperfusion injury in rats. *Ren Fail* 38:614-621. 10.3109/0886022x.2016.1149770

Wang X, Pan X, and Song J. 2010. AMP-activated protein kinase is required for induction of apoptosis and epithelial-to-mesenchymal transition. *Cell Signal* 22:1790-1797. 10.1016/j.cellsig.2010.07.008

Weitz M, Portz S, Laube GF, Meerpohl JJ, and Bassler D. 2016. Surgery versus non-surgical management for unilateral ureteric-pelvic junction obstruction in newborns and infants less than two years of age. *Cochrane Database Syst Rev* 7:Cd010716. 10.1002/14651858.CD010716.pub2

Zhang D, Sun L, Xian W, Liu F, Ling G, Xiao L, Liu Y, Peng Y, Haruna Y, and Kanwar YS. 2010. Low-dose paclitaxel ameliorates renal fibrosis in rat UUO model by inhibition of TGF-beta/Smad activity. *Lab Invest* 90:436-447. 10.1038/labinvest.2009.149

Zhao Q, Yang Y, Wang CL, Hou Y, and Chen H. Screening and identification of the differential proteins in kidney with complete unilateral ureteral obstruction.

Table 1(on next page)

qRT-PCR primer sequences of rat

Table 1 qRT-PCR primer sequences of rat

Gene	R-Sequence(5'→3')	F-Sequence(5'→3')
AMPKα2	CACTTGACCGAGGTCTGTGGA	TGAGCTTACAGCTTTACCTGGTTGA
ETS1	TGAACTCATTCACAGCCCACATC	ATGTCCCAGGCACTGAAAGCTAC
RPS6KA1	GTGCCAGCTCAGCCAGGTAA	CAGACCGAGGGCAAGCTCTA
CREB1	GCACTAAGGTTACAGTGGGAGCAGA	ACAGTTCAAGCCCAGCCACAG
CRK	GAAGTGACCTCGTTTGCCATTACA	CAGAAGCGAGTCCCTAATGCCTAC
HRAS	TTCCTTCCTTCCCTCCTCTTTC	CTGCAGTCAGTCATGTCCTTTGT
β-actin	CAGAGGCATACAGGGACAACAA	CCTAAGGCCAACCGTGAAAA

Table 2(on next page)

Genes inhibited in the ERK/MAPK signaling pathway after the AMPKα2 knockdown

Table 2 Genes inhibited in the ERK/MAPK signaling pathway after the AMPKα2 knockdown

Gene symbol	Gene Name
PIK3CA	phosphatidylinositol-4,5-bisphosphate 3-kinase catalytic subunit alpha
PPP2CA	protein phosphatase 2 catalytic subunit alpha
DUSP6	dual specificity phosphatase 6
HRAS	HRas proto-oncogene, GTPase
PPP1CB	protein phosphatase 1 catalytic subunit beta
CRK	CRK proto-oncogene, adaptor protein
KRAS	KRAS proto-oncogene, GTPase
PPP1R14B	protein phosphatase 1 regulatory inhibitor subunit 14B
KSR1	kinase suppressor of ras 1
SHC1	SHC adaptor protein 1
LAMTOR3	late endosomal/lysosomal adaptor, MAPK and MTOR activator 3
CREB1	cAMP responsive element binding protein 1
PPM1L	protein phosphatase, Mg2+/Mn2+ dependent 1L
PRKCA	protein kinase C alpha
NRAS	NRAS proto-oncogene, GTPase
ATF1	activating transcription factor 1
GRB2	growth factor receptor bound protein 2

PPP2R5D	protein phosphatase 2 regulatory subunit B'delta
CREBBP	CREB binding protein
PRKAR2A	protein kinase cAMP-dependent type II regulatory subunit alpha
MKNK2	MAP kinase interacting serine/threonine kinase 2
RAP1A	RAP1A, member of RAS oncogene family
ELF2	E74 like ETS transcription factor 2
H3F3A/H3F3B	H3 histone family member 3A
TLN2	talin 2
PRKAR2B	protein kinase cAMP-dependent type II regulatory subunit beta
PRKCI	protein kinase C iota
RRAS2	RAS related 2
Pak2	p21 protein (Cdc42/Rac)-activated kinase 2
PAK2	p21 (RAC1) activated kinase 2
PIK3CB	phosphatidylinositol-4,5-bisphosphate 3-kinase catalytic subunit beta
RPS6KA1	ribosomal protein S6 kinase A1
ELK3	ELK3, ETS transcription factor
PPP2R1B	protein phosphatase 2 scaffold subunit Abeta

ESR1	estrogen receptor 1
ETS1	v-ets erythroblastosis virus E26 oncogene homolog-1

Figure 1

Morphological changes in NRK-52E cells before and after TGF-β1 treatment.

TGF-β1 (10 ng/mL) induced morphological changes in NRK-52E cells after 24 h, which changed from typical round and polygonal to fusiform, suggesting that the EMT occurred (magnification: 200×).

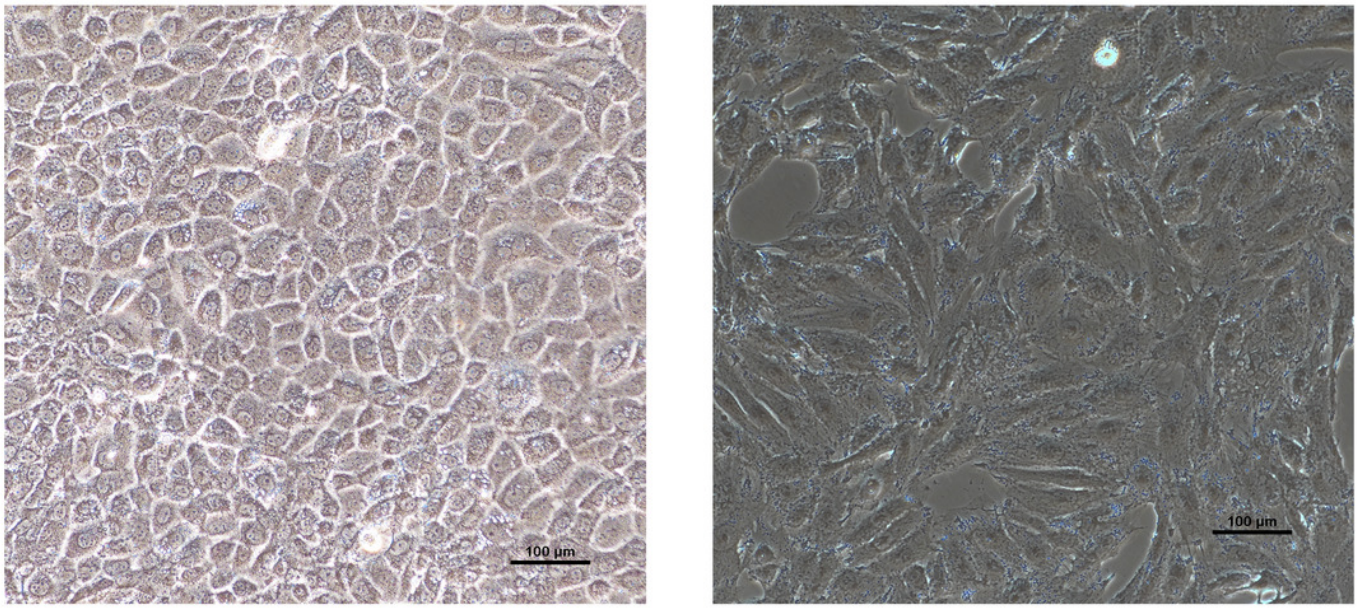

Control TGF-β1-treated

Figure 2

Western blot analysis of the EMT-related proteins α-SMA, vimentin, and E-cadherin in four groups.

Blot is representative of at three independent experiments; GAPDH was used as a loading control; Ctrl: control; one-way ANOVA, *, **, $^{\#}$, $^{\#\#}$, $^{\&}$, $^{\&\&}$, $P<0.05$.

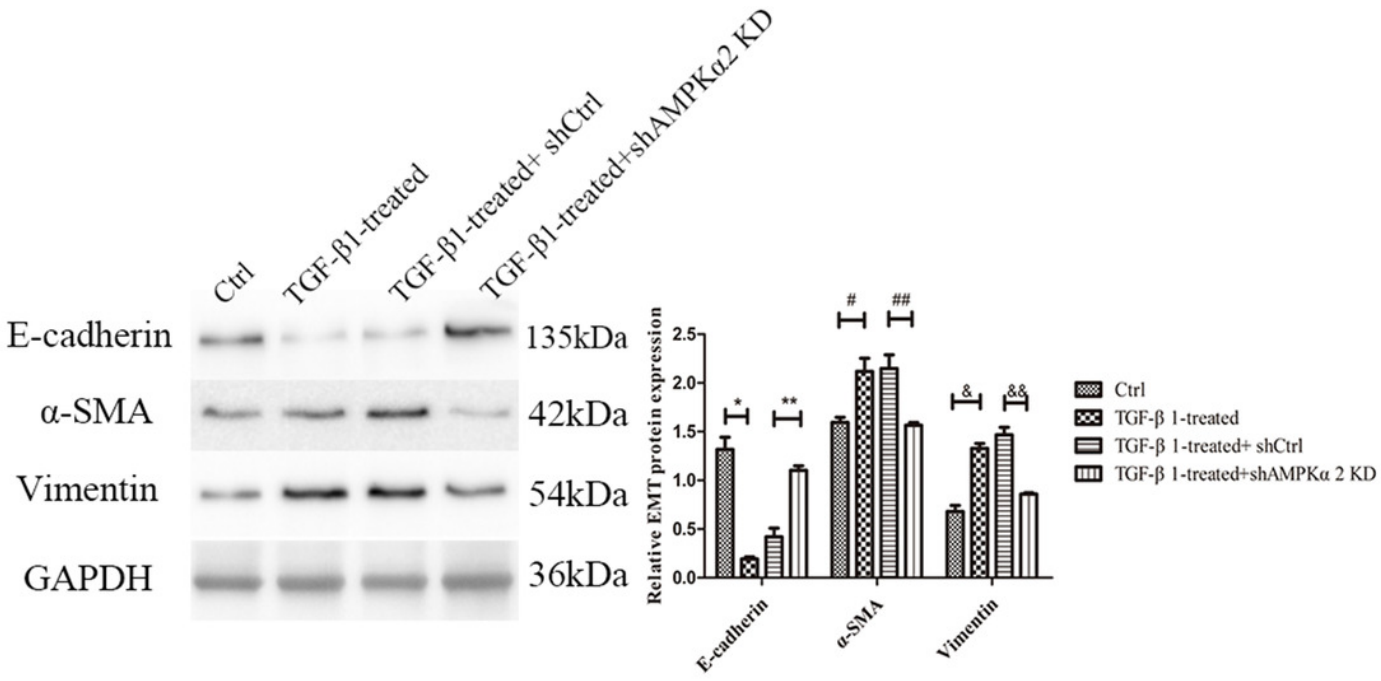

Figure 3

Expression of AMPKα2 protein and mRNA in immunofluorescence and qRT-PCR.

(A) After TGF-β1 treatment of NRK-52E cells, AMPKα2 was mainly expressed in the cytoplasm and nucleus of NRK-52E cells (magnification: 200×). (B) Analysis of AMPKα2 mRNA between control and TGF-β1 treated groups by qRT-PCR. housekeeping gene β-actin as endogenous control; n=3; Ctrl: control; Student's t-test , * P<0.05.

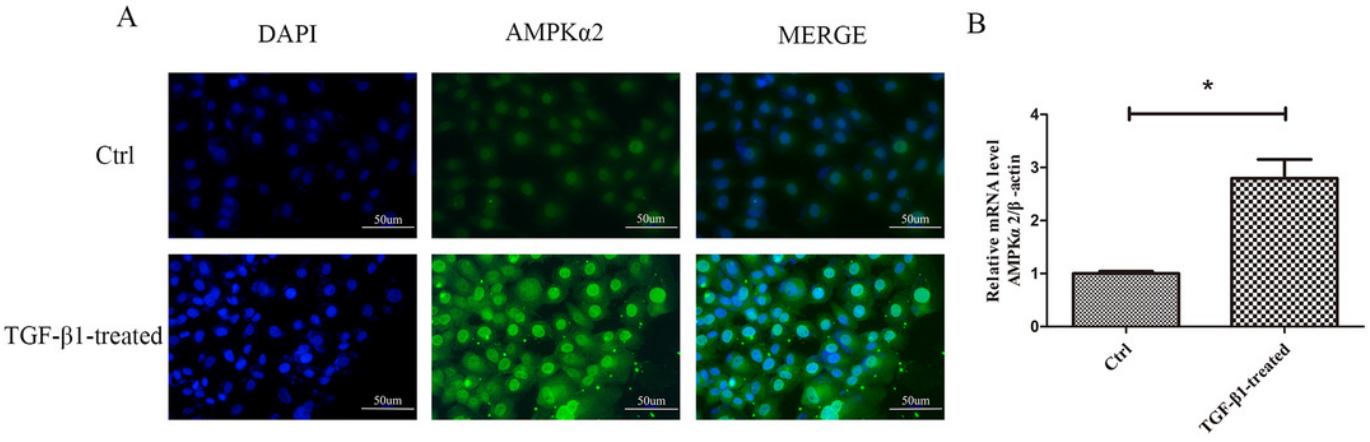

Figure 4

Western blot analysis of AMPKα2.

Blot is representative of at three independent experiments. GAPDH was used as a loading control; Ctrl: control; one-way ANOVA, *, **, P<0.05.

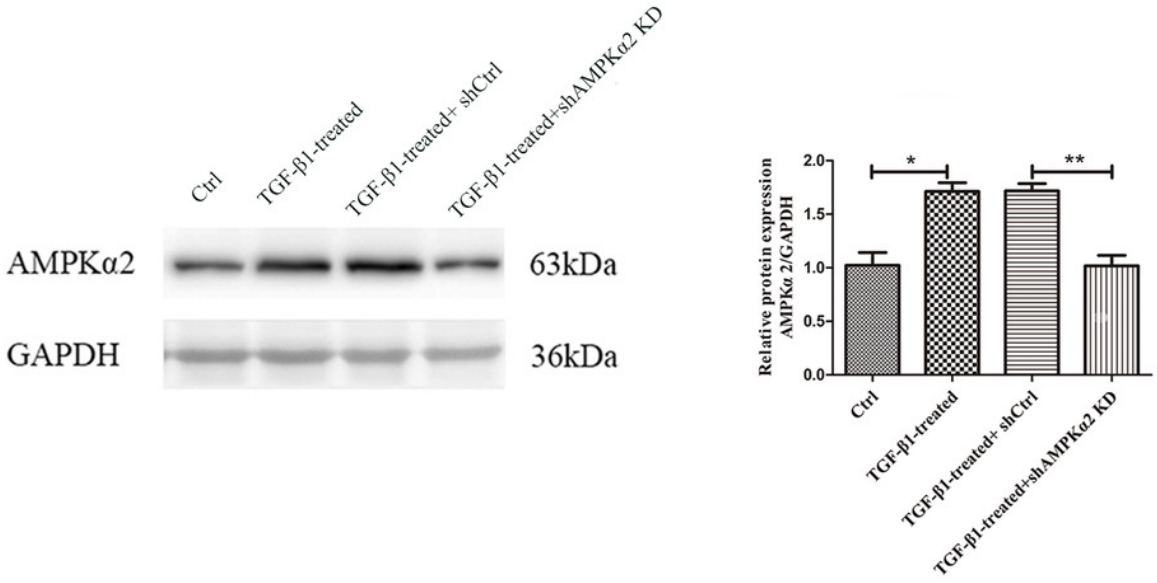

Figure 5

Transfection and knock- efficiency of AMPKα2 short hairpin RNA and control lentivirus.

(A) The EMT-derived NRK-52E cells after 72 h of transfection with AMPKα2 short hairpin RNA and control lentivirus, GFP expression was observed in the cells, indicating successful transfection (magnification: 200×). (B) Analysis of AMPKα2 mRNA between TGF-β1-treated+shCtrl and TGF-β1-treated+sh AMPKα2KD group by qRT-PCR; housekeeping gene β-actin as endogenous control; n=3; Ctrl: control; Student's t-test, $^{*}P<0.05$.

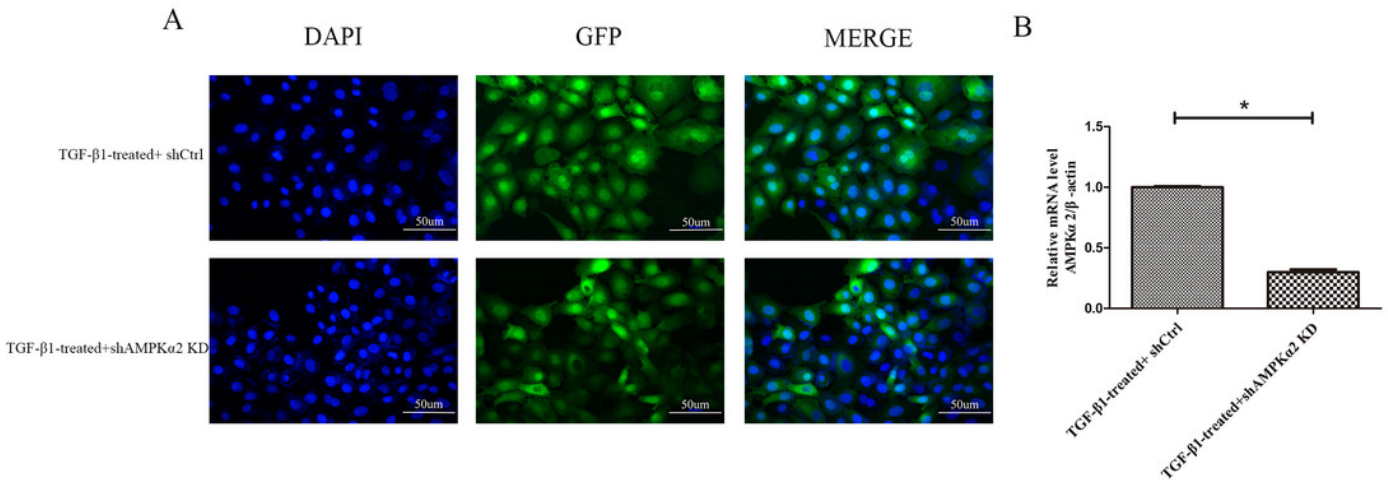

Figure 6

Rat gene chip results and IPA.

(A) Differential gene expression heat map in rat gene chip. (B) Significant enrichment of differential genes in the classical pathway. Orange label indicates pathway activation (z-score>0), blue label indicates pathway suppression (z-score<0), and shades of orange and blue (or absolute value of z-score) represent levels of activation or inhibition. ERK/MAPK signaling was significantly inhibited with a z-score of -3.550. (C) ERK/MAPK signaling was significantly inhibited. Red indicates significant gene upregulation in the experimental results and green indicates significant gene downregulation.

A

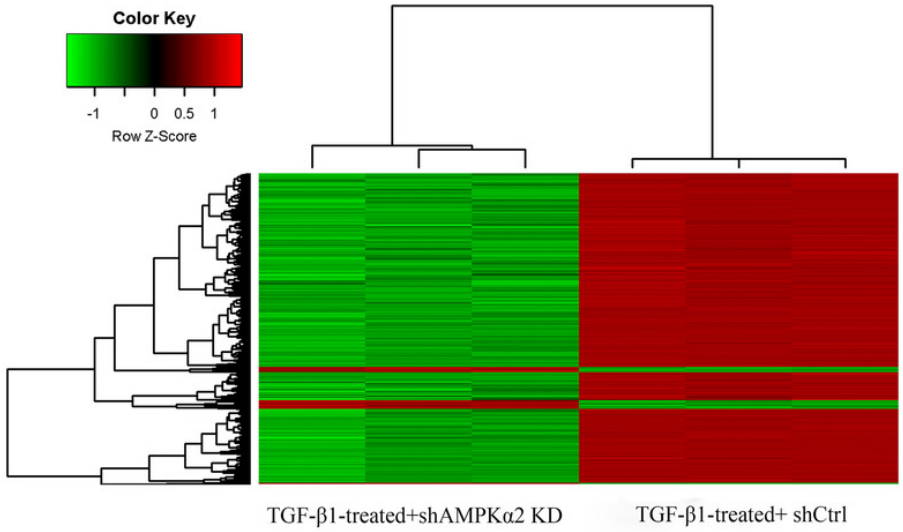

B

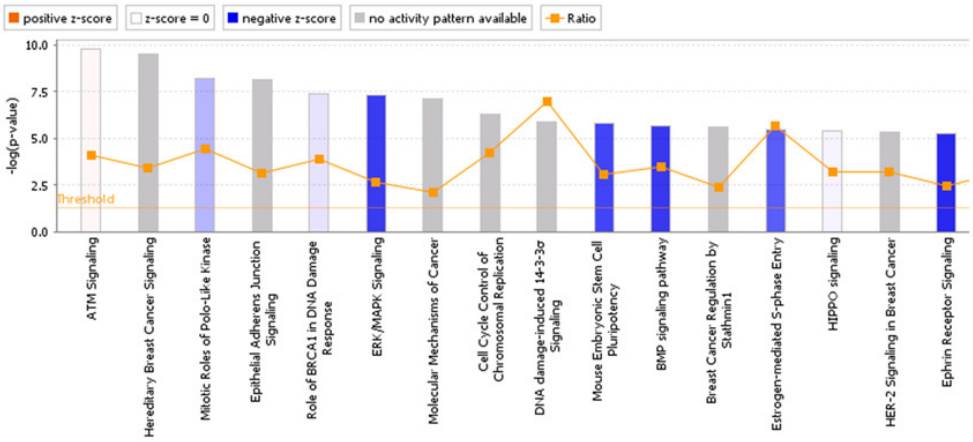

C

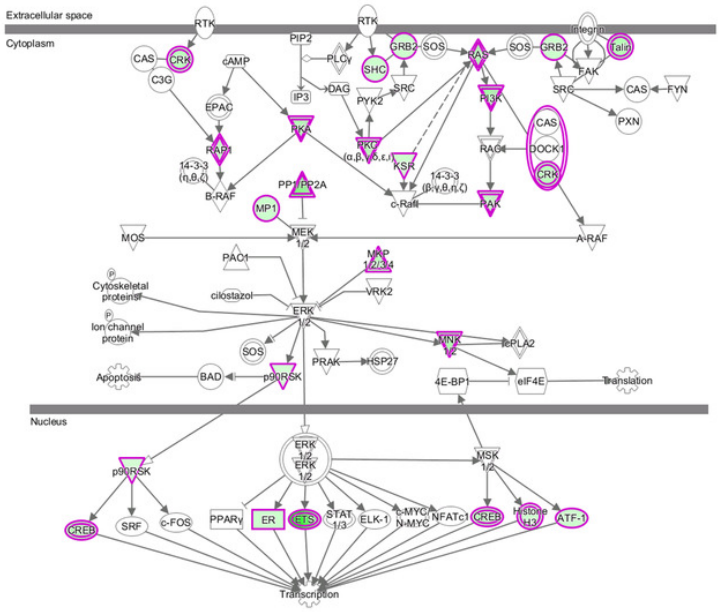

Figure 7

Differentially expressed mRNA levels in four groups were verified by qRT-PCR.

Housekeeping gene β-actin as endogenous control; n=3; Ctrl: control; one-way ANOVA, *, **, $P<0.05$.

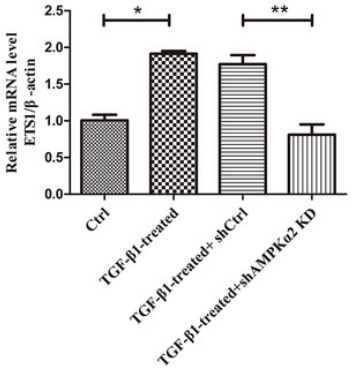
Relative mRNA level
ETS1/β -actin
2.5
2.0
1.5
1.0
0.5
0.0
*
**
Ctrl
TGF-β1-treated
TGF-β1-treated+ shCtrl
TGF-β1-treated+shAMPKα2 KD

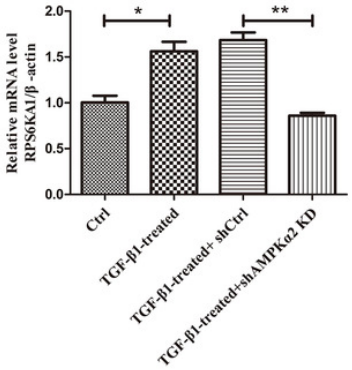
Relative mRNA level
RPS6KA1/β -actin
2.0
1.5
1.0
0.5
0.0
*
**
Ctrl
TGF-β1-treated
TGF-β1-treated+ shCtrl
TGF-β1-treated+shAMPKα2 KD

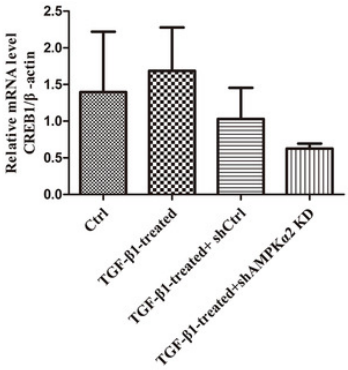
Relative mRNA level
CREB1/β -actin
2.5
2.0
1.5
1.0
0.5
0.0
Ctrl
TGF-β1-treated
TGF-β1-treated+ shCtrl
TGF-β1-treated+shAMPKα2 KD

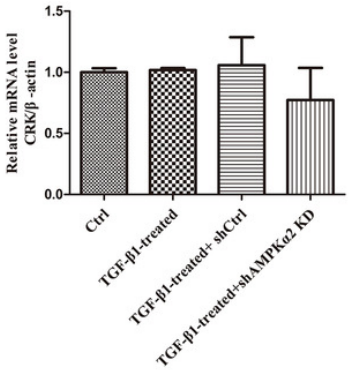
Relative mRNA level
CRK/β -actin
1.5
1.0
0.5
0.0
Ctrl
TGF-β1-treated
TGF-β1-treated+ shCtrl
TGF-β1-treated+shAMPKα2 KD

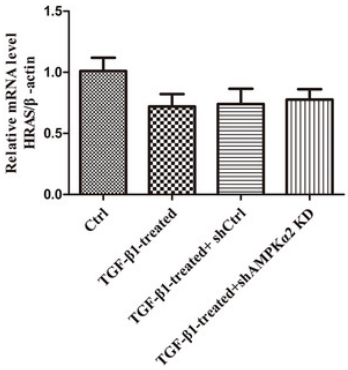
Relative mRNA level
HRAS/β -actin
1.5
1.0
0.5
0.0
Ctrl
TGF-β1-treated
TGF-β1-treated+ shCtrl
TGF-β1-treated+shAMPKα2 KD

Figure 8

Western blot analysis of ETS1.

Blot is representative of at three independent experiments; GAPDH was used as a loading control; Ctrl: control; one-way ANOVA, *, **, P<0.05.

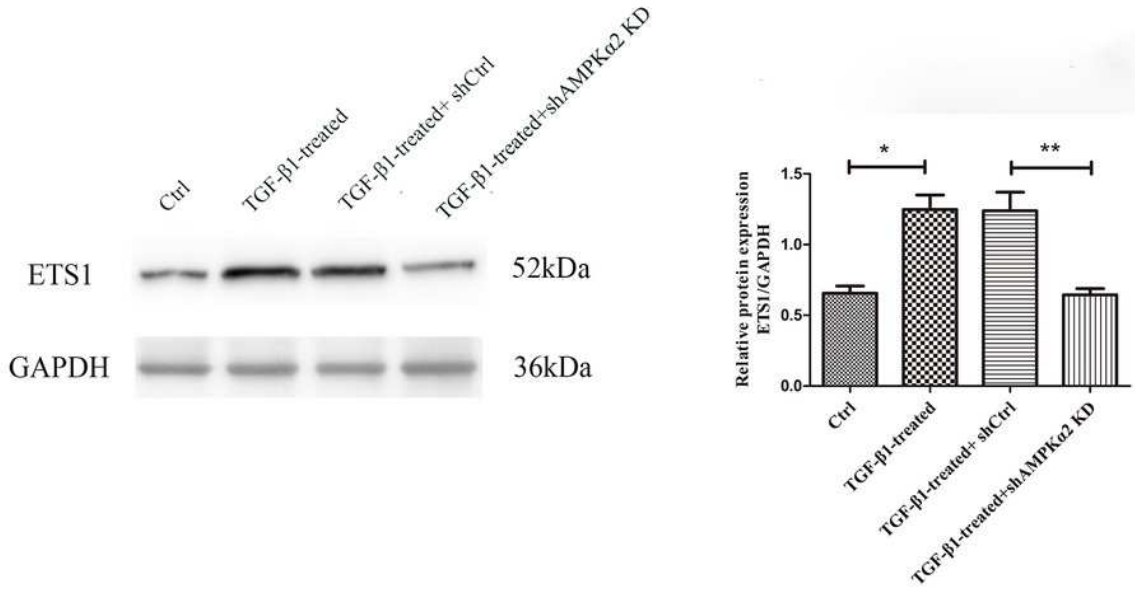

Figure 9

Western blot analysis of RPS6KA1.

Blot is representative of at three independent experiments; GAPDH was used as a loading control; Ctrl: control; one-way ANOVA, *, **, P<0.05.